International Nano Letters
a SpringerOpen Journal

ORIGINAL ARTICLE Open Access

Free energies, kinetics, and photoelectron-transfer properties, and theoretical and quantitative structural relationship studies of [SWCNT(5,5)-armchair-C_nH_{20}][*R*] (*R* = η^2-C_mPd(dppf), η^2-C_mPd(dppr), and η^2-C_mPd(dppcym)$_2$, *n* = 20 to 300 and *m* = 60 and 70) nanostructure complexes

Avat Arman Taherpour[1*] and Zahra Talebi-Haftadori[2]

Abstract

Metal complexes containing one or several bis(triorganylphosphine)palladium fragments attached to the C_{60} core and coordinated in olefinic η^2 mode have been previously described. The number of carbon atoms of the single-walled carbon nanotubes (SWCNTs) is the useful numerical and structural electrochemical properties contributing to the relationship between the structures of the η^2-C_mPd(dppf), η^2-C_mPd(dppr), and η^2-C_mPd(dppcym)$_2$ (*m* = 60 and 70) ligands (A to E) and [SWCNT(5,5)-armchair-C_nH_{20}] (*n* = 20 to 190) 1 to 18 and the production of the [SWCNT(5,5)-armchair-C_nH_{20}][*R*] (*R* = η^2-C_mPd(dppf), η^2-C_mPd(dppr), and η^2-C_mPd(dppcym)$_2$, *n* = 20 to 300 and *m* = 60 and 70) complexes 30 to 174. In this study, the relationship between the number of carbon atoms index and the first and second free energies of electron transfer ($\Delta G_{et(n)}$, *n* = 1,2) using the Rehm-Weller equation based on the first and second oxidation potentials ($^{ox}E_1$ and $^{ox}E_2$) of A to E for the predicted complexes 30 to 174 between 1 and 29 with exohedral metallofullerenes A to E, as [SWCNT(5,5)-armchair-C_nH_{20}][*R*] (*R* = η^2-C_mPd(dppf), η^2-C_mPd(dppr), and η^2-C_mPd(dppcym)$_2$, *n* = 20 to 300 and *m* = 60 and 70) 30 to 174 was assessed. Here, the first and second free activation energies of electron transfer and the wavelengths of the electromagnetic photons in the photoelectron transfer process, $\Delta G^{\#}_{et(n)}$ and $\lambda_{(n)}$ (nm), respectively, for 30 to 174 in accordance with the Marcus theory and Planck's equation were also calculated.

Keywords: Exohedral metallofullerenes, Pd complexes, Single-walled nanotubes, Free energy of electron transfer, Photoelectron transfer, Marcus theory, Planck's equation

Background

The first metal complexes containing one or several bis(triorganylphosphine)platinum fragments attached to the C_{60} core and coordinated in the olefinic η^2 mode were described in 1991 [1-3], revealing that fullerenes, at least buckminsterfullerene C_{60}, can function as ligands in reactions with transition metals. Electronic structures of exohedral palladium complexes of [60] and [70] fullerenes with diphenylphosphinoferrocenyl, diphenylphosphinoruthenocenyl, and diphenylphosphinocymantrenyl ligands were studied by cyclic voltammetry and semi-empirical quantum chemical calculations in 2004 [1]. The probable sites of the electronic changes in these complexes under electrochemical oxidation and reduction have also been determined [1-4].

The bulk of fullerene metal complexes consist of heteroligand complexes. The only exceptions known to date are polymeric homoligand complexes of C_{60} with palladium or platinum, which are prepared by the direct reaction of fullerene with zero-valent complexes of these

* Correspondence: avatarman.taherpour@gmail.com
[1]Department of Organic Chemistry, Faculty of Chemistry, Razi University, P.O. Box 67149–67346, Kermanshah, Iran
Full list of author information is available at the end of the article

metals with a weakly bound ligand, dibenzylideneacetone [1-8]. The platinum and palladium complexes $(C_{60})M_x$ (M = Pt and Pd) can also be prepared from the Pt(0) and Pd cyclooctadiene complexes. Two C_{60} molecules are bound to the metal atom in η^2 mode. However, instead of separate $(C_{60})_2M$ molecules, a polymeric chain is formed, which is probably indicative of enhanced reactivity (with respect to ligand-free palladium) of the other fullerene double bonds upon coordination of one bond. If an excess of the $M(0)$ compound is present, the specific content of the metal increases [1-8]. According to elemental analysis, the insoluble precipitates have compositions of $(C_{60})Pd_x$, where x = 1, 2, 3, and more. Some free metal is always present. C_{60} molecules are presumably linked by metal atoms into one-dimensional chains or two- and three-dimensional frameworks. The palladium (platinum) fullerene polymer reacts heterogeneously with P ligands (tertiary phosphines or tertiary phosphites) in solution to give the $C_{60}ML_2$ complexes, which can also be synthesized by other methods [1-8]. The electrochemical synthesis of the $(\eta^2\text{-}C_{60}M(PPh_3)_2$ (M = Pt, Pd) complexes was performed by reacting the dianion of C_{60}^{2-} prepared by electrochemical reduction (at a Pt electrode in a toluene-acetonitrile solution in the presence of Bu_4NBF_4 as the supporting electrolyte) with the ML_2Cl_2 complex or with a divalent metal chloride in the presence of triphenylphosphine [1-4]. The palladium derivatives of C_{60} and C_{70} with cymantrenyldiphenylphosphine ligand were prepared in a similar way [7,8]. A series of new exohedral Pd(0) complexes with C_{60} and C_{70} fullerenes containing bisdiphenylphosphinoferrocene (dppf), bisdiphenylphosphinoruthenocene (dppr), or two diphenylphosphinocymantrene (dppcym) molecules as stabilizing ligands have been synthesized. These complexes contain a strongly electron-withdrawing fullerene cage and a metallocene group, which can be either electron releasing (ruthenocene) or electron withdrawing (cymantrene) and is linked with the cage through a bisdiphenylphosphine palladium bridge. The electrochemical pattern is impeded because the bisdiphenylphosphine palladium fragment linking these terminal groups is also redox active [1-8].

Metal complexes with fullerenes have attracted attention due to the prospects of their application in catalysis, in materials for nonlinear optics, for designing artificial photosynthesis systems, and in the development of supra- and nanomaterials [4]. More specifically, metal-fullerene interactions are of particular importance. Platinum was the first metal found to form π-complexes with fullerenes. However, evidence for the existence of similar complexes for palladium was obtained soon thereafter. The most practical preparation of palladium η^2 complexes appeared to be by direct synthesis using $Pd_2(dba)_3$, fullerene, and a free phosphine ligand. Almost all known complexes of fullerenes with an undisturbed electronic system involve only η^2 coordination, which is typical of an isolated olefinic double bond. The η^2 coordination is probably due to the nonplanar surface geometry, which makes the axes of the pseudo-π-orbitals nonparallel and, thus, hampers their bonding to metal orbitals [1-8].

Nanotubes of type (n,n) are called *armchair nanotubes* because of their 'W' shape perpendicular to the tube axis. They are symmetrical along the tube axis, with a short unit cell (0.25 nm or 2.5 Å) that is repeated along the entire section of a long nanotube. All other nanotubes are called *chiral nanotubes* and have longer unit cell sizes along the tube axis [9-11]. The simplest type of nanotube is a cylindrical structure, which conceptually could be formed by folding and gluing a pair of opposite sides of a rectangular graphite sheet [9-24]. If both ends are capped, it will have at least two pentagons and be a type of fullerene. Nanotubes are large, linear fullerenes with aspect ratios as large as 103 to 105 [11]. The walls of such tubes can have various sizes of polygons [25]. Although many nanoscale fullerene materials occur regularly in applications, controlled production of numerous fullerenes and nanotubes with well-defined characteristics has not yet been achieved [16-19,25].

Carbon nanotubes possess many special properties, such as an open mesoporous structure, high electrical conductivity and chemical stability, and extremely high mechanical strength and modulus [11,19-21]. These properties not only help in the transportation of ions but also facilitate the charging of the double layer and confer advantages in the development of electrochemical capacitors [22]. Single-walled carbon nanotubes have been recognized as potential electrode materials for electrochemical capacitors [23,24].

One of the most widely recognized structures of nanotubes is the (5,5) tube, which can be built by successively adjoining sections of ten C atoms. In the infinite tube, the periodic unit cell has two sections, each consisting of 20 C atoms [9]. The electronic structures and electrical properties of single-walled nanotubes can be simulated from those of a graphite layer (graphene sheet) [19-24].

Figure 1 shows the (5,5) *armchair* form with the imaginary structures of the η^2–C_mPd(dppf), η^2–C_mPd(dppr), and η^2–C_mPd(dppcym)$_2$ (m = 60 and 70) ligands (A to E) and 1 to 174 as [SWCNT(5,5)-armchair-C_nH_{20}][R] (R = η^2-C_mPd(dppf), η^2-C_mPd(dppr), and η^2-C_mPd(dppcym)$_2$, n = 20 to 300 and m = 60 and 70) 30 to 174. The nanotubes may not contain any hydrogen atoms (there is no hydrogen in the electric arc technique), and the nanotubes can be easily closed at both ends.

Electronic structures of tubular aromatic molecules derived from the metallic (5,5) armchair SWCNT for $C_{20}H_{20}$ up to $C_{210}H_{20}$ (see Figure 1) were reported by Zhou et al. in 2004 [9]. The authors considered how the

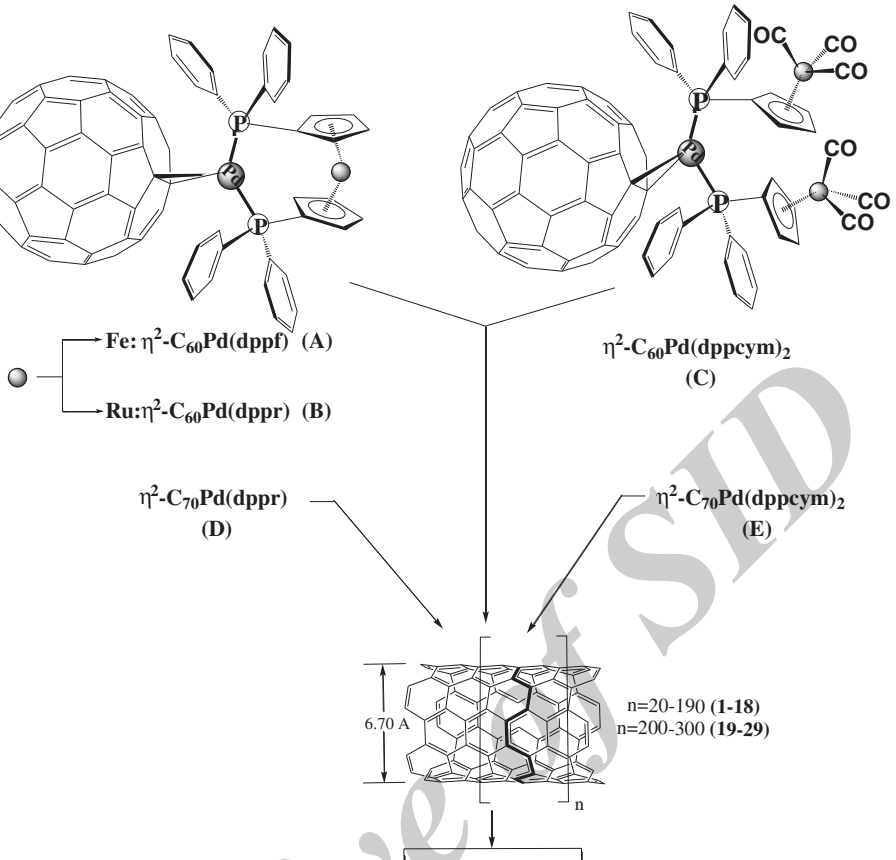

Complexes of **1-29** with **A-E**	n=20-190	n=200-300
[SWCNT(5,5)-Armchair-C_nH_{20}].[**A**]	**30-47**	**120-130**
[SWCNT(5,5)-Armchair-C_nH_{20}].[**B**]	**48-65**	**131-141**
[SWCNT(5,5)-Armchair-C_nH_{20}].[**C**]	**66-83**	**142-152**
[SWCNT(5,5)-Armchair-C_nH_{20}].[**D**]	**84-101**	**153-163**
[SWCNT(5,5)-Armchair-C_nH_{20}].[**E**]	**102-119**	**164-174**

Figure 1 Schemes. A to **E** and [SWCNT(5,5)-armchair-C_nH_{20}][*R*] (*R* = η^2-C_mPd(dppf), η^2-C_mPd(dppr), and η^2-C_mPd(dppcym)$_2$, *n* = 20 to 300 and *m* = 60 and 70) complexes.

electronic structures of short molecular sections of the (5,5) tube relate to, differ from, and asymptotically approach those of an infinite metallic tube [9]. Some of the structural and electronic properties were investigated, such as the ionization potential, electron affinity, Fermi energy, chemical hardness, and relative energetic stability. All of these metrics show the length periodicity in the frontier orbital (i.e., highest occupied molecular orbital-lowest unoccupied molecular orbital) gap, in contrast to the optical 'charge transfer' transition and the static axial polarizability [9]. The (5,5) nanotubes have two types of symmetry. For nanotubes with odd identification numbers (1 to 17), the point group is D_{5d}, whereas nanotubes with even identification numbers (2 to 18) have a point group of D_{5h}. Static and time-dependent density function theory calculations were used to independently optimize the structure for neutral, cationic, and anionic complexes [9]. The hybrid nonlocal Becke, three-parameter, Lee-Yang-Parr (B3LYP) function was applied [9].

Infinite-length SWCNTs are π-bonded aromatic structures that can be either semi-conducting or metallic, depending upon the diameter and helical angle of the SWCNTs. In a pioneering 1992 DFT calculation, Mintmire et al. predicted that the infinite length (5,5) armchair SWCNT (6.70 Å diameter) would be metallic with a very low transition temperature separating the uniform (high-temperature) structure from the Peierls bond alternating (low-temperature) structure [23,26]. This specific SWCNT is the elongated tube of the C_{60}, C_{70}, etc. molecular family [9]. Most of the previous studies have dealt with C_{60}@SWCNT and C_{70}@SWCNT structures [18,27-30].

The diameter sizes of C_{60} and [SWCNT(5,5)-armchair-C_nH_{20}] 1 to 18 were reported to be 6.70 and 6.94 Å, respectively [28-30]. With these diameters, C_{60} and larger fullerenes cannot be encapsulated inside the [SWCNT(5,5)-armchair-C_nH_{20}] in the structure of C_n@[SWCNT(5,5)-armchair-C_nH_{20}].

Any extrapolation of results from one compound to other compounds must take into account considerations based on a Quantitative Structural Analysis Relationship Study, which mostly depends on the similarity of the physical and chemical properties of the compounds in question. Numerous studies in the above areas have also used topological indices [31-35]. In previous studies, the relationship between the D_{UI} index and electron affinity, reduction potential ($^{Red.}E_1$) of [SWCNT(5,5)-armchair-C_nH_{20}] as well as the free energy of electron transfer (ΔG_{et}) between [SWCNT(5,5)-armchair-C_nH_{20}] structures and fullerene C_{60} in C_{60}@[SWCNT(5,5)-armchair-C_nH_{20}] complexes was investigated [28]. In some studies, the relationship between the D_{UI} index and the free energy of electron transfer (ΔG_{et}) using the Rehm-Weller equation based on the first oxidation potential ($^{ox}E_1$) of $Sc_2@C_{84}$ and $Er_2@C_{82}$ for the predicted supramolecular complexes between SWCNT(5,5)-armchair-C_nH_{20} and the endohe dral metallofullerenes $Sc_2@C_{84}$ and $Er_2@C_{82}$ as [$M_2@Cx$]@[SWCNT(5,5)-armchair-C_nH_{20}] (M = Er and Sc, x = 82 and 84) [28-30,36] was assessed.

To characterize the structural properties of the π-bonds, we investigated the relationship between the number of carbon atoms of the SWCNT (C_n) index and electron affinity, $^{Red.}E_1$ of [SWCNT(5,5)-armchair-C_nH_{20}] 1 to 18 (and extension of the results to 19 to 29) as well as the first and second free energies of electron transfer ($\Delta G_{et(n)}$, n = 1,2) using the Rehm-Weller equation [36] based on the first and second oxidation potential ($^{ox}E_1$ and $^{ox}E_2$) of the η^2-C_mPd(dppf)), η^2-C_mPd(dppr), and η^2-C_mPd(dppcym)$_2$ (m = 60 and 70) ligands (A to E) for the predicted [SWCNT(5,5)-armchair-C_nH_{20}][R] (R = η^2-C_mPd(dppf), η^2-C_mPd(dppr), and η^2-C_mPd(dppcym)$_2$, n = 20 to 300 and m = 60 and 70) supramolecular complexes 30 to 174. We also calculated the first and second activation free energies of electron transfer and the wavelengths of the electromagnetic photons in the photoelectron transfer process, $\Delta G^{\#}_{et(n)}$, and $\lambda_{(n)}$ (nm) using the Marcus theory, Planck's equation, and the equations based on the first and second oxidation potentials ($^{ox}E_1$ and $^{ox}E_2$) of A-E for the predicted supramolecular complexes 30 to 174. The Marcus theory is based on the traditional Arrhenius equation for the rates of chemical reactions in two ways. First, it provides a formula for the pre-exponential factor in the Arrhenius equation, based on the electronic coupling between the initial and final states of the electron-transfer reaction (i.e., the overlap of the electronic wave functions of the two states). Second, it provides a formula for the activation energy, based on a parameter called the *reorganization energy*, as well as the *Gibbs* free energy. The reorganization energy is defined as the energy required to reorganize the structure of the system from initial to final coordinates without changing the electronic state [37-42].

Although electrons are commonly described as residing in electron bands in bulk materials and electron orbitals in molecules, the following description will be described in molecular terms. When a photon excites a molecule, an electron in a ground state orbital can be excited to a higher energy orbital. This excited state leaves a vacancy in a ground state orbital that can be filled by an electron donor. An electron is produced in a high-energy orbital and can be donated to an electron acceptor. Photo-induced electron transfer is an electron transfer that occurs when certain photoactive materials interact with light, including semiconductors that can be photo-activated, such as many solar cells, biological systems like those used in photosynthesis, and small molecules with suitable absorptions and redox states [36-42].

Methods

The number of carbon atoms of the SWCNTs (C_n) was used as a structural index (1 to 29). All mathematical and graphing operations were performed using *MATLAB-7.4.0 (R2007a)* and *Microsoft Office Excel 2003* programs. The number of carbon atoms in the SWCNTs (C_n) is a useful numerical and structural value in characterizing the empty fullerenes. However, we used other selected indices and the best results and equations for extending the physicochemical and electrochemical data.

The Rehm-Weller equation estimates the free energy change between an electron donor (D) and an acceptor (A) as

$$\Delta G_{et}^{\circ} = e[E_D^{\circ} - E_A^{\circ}] - \Delta E^* + \omega_1, \quad (1)$$

where e is the unit electrical charge, E_D° and E_A° are the reduction potentials of the electron donor and acceptor, respectively, ΔE^* is the energy of the singlet or triplet excited state, and ω_1 is the work required to bring the donor and acceptor within the electron transfer (ET) distance. The work term in this expression can be considered to be '0' in so far as an electrostatic complex exists before the electron transfer [36].

The Marcus theory of electron transfer implies rather weak (<0.05 eV) electronic coupling between the initial (locally excited (LE)) and final (ET) states, and presumes that the transition state is close to the crossing point of the LE and CT terms. The value of the electron transfer rate constant k_{et} is controlled by the activation free energy $\Delta G^{\#}_{et}$, which is a function of the reorganization energy (l/4) and the electron transfer driving force ΔG_{et}:

$$\Delta G_{et} = (l/4)(1 + \Delta G_{et}/l)^2, \quad (2)$$

$$k_{et} = k_0 \exp(-\Delta G_{et}/RT). \quad (3)$$

The reorganization energy of organic molecules ranges from 0.1 to 0.3 eV. In this study, we used the minimum amount of reorganization energy [37-42].

To calculate the maximum wavelengths ($\lambda_{(n)}$; n = 1 to 2 of the electromagnetic photon for the electron transfer process in the nanostructure supramolecular complexes, we used Planck's formula:

$$\Delta G_{et} = \Delta E = h.c/\lambda_{(n)}. \quad (4)$$

In this study, this formula was also used to calculate the activation free energy of the electron transfer process [43].

Results and discussion

The electronic structures of the exohedral palladium complexes of [60]_ and [70]_fullerenes with diphenylphos phinoferrocenyl, diphenylphosphinoruthenocenyl, and diphenylphosphinocymantrenyl ligands (η^2-C_mPd(dppf), η^2-C_mPd(dppr), and η^2-C_mPd(dppcym)$_2$ (m = 60 and 70) (A to E), respectively) were studied by cyclic voltammetry and semi-empirical quantum chemical calculations. The C_{60}Pd(dppf), C_{60}Pd(dppcym)$_2$, C_{60}Pd(dppr), C_{70}Pd(dppr), and C_{70}Pd(dppcym)$_2$ complexes were synthesized using the Schlenk technique by a previously described method [1,2,5,6]. The reaction required equivalent amounts of the respective fullerene, $Pd_2(dba)_3$ complex (where dba is dibenzylideneacetone) and phosphine ligand under argon. Measurements of ^{Ox}E and ^{Red}E have been previously reported [1,2]. Voltammograms were recorded with 0.15 $MBu^n_4NBF_4$ as a supporting electrolyte in *ortho*-dichlorobenzene at 20°C in a 10-mL electrochemical cell vs. Ag/AgCl/KCl. Oxygen was removed by passing dry argon through the cell [1,2]. The CV curves were recorded on a stationary graphite electrode with sweep rates of 100 and 200 mV s^{-1}. The potentials of the peaks, which were often poorly pronounced in the CV curves, were determined [1,2]. The first and second reported oxidation potential ($^{ox}E_1$ and $^{ox}E_2$ in volt) states of A to E are as follows [1,2]:

$^{ox}E_1$: + 0.87(A), + 0.82(B), + 1.03(C), + 0.86(D), + 1.03 (E) [16]
$^{ox}E_2$: + 1.22(A), + 1.16(B), + 1.44(C), + 1.20(D), + 1.35 (E) [16]

The energy (E_a) is released upon the attachment of an electron to an atom or a molecule (A), resulting in the formation of the negative ion A^-, i.e., $A + e^- \rightarrow A^- + E_a$. As in the case of the ionization potential, the adiabatic electron affinity (E_{aa}) and vertical electron affinity can be defined. The adiabatic E_a is equal to the difference between the total energies of a neutral system (A) and the corresponding anion (A^-). The vertical A_X is equal to the difference between the total energies of A and the anion A^- in the equilibrium geometry of A [44]. The free energy of this reaction ($\Delta E_s(A \rightarrow A^-)$) corresponds to the absolute redox energy for the above process. The free energy of an electron (e^-) at rest in the gas phase is set to zero [45,46]. The redox energy of the reaction ($A + e^- \rightarrow A^- + E_a$) can be calculated using a thermodynamic equation (see Equation 5). In this equation, $\Delta G_s(A)$ and $\Delta G_s(A^-)$ are the solvation energies of molecule A and its anion A^-, respectively, and $\Delta E_g(A \rightarrow A^-)$ is the energy difference between molecule A and its anion (which is defined as the redox energy in the gas phase). Based on this thermodynamic cycle, we can obtain $\Delta E_s(A \rightarrow A^-)$, the absolute redox energy [45,46]:

$$\Delta E_s(A \rightarrow A^-) = \Delta E_g(A \rightarrow A^-) + \Delta G_s(A) - AG_s(A^-). \quad (5)$$

By calculating the gas phase energies and solvation energies of molecule A and its anion A^-, the absolute redox potential (scaled) of molecule A in solution can be derived. A scaling coefficient that translates electron affinity into standard redox potentials can be extracted [44-46]. As seen in the results of [16], the static TD-DFT and independently optimized structure were used to calculate the physicochemical and electronic structure of tubular aromatic molecules derived from the metallic (5,5) armchair single-walled carbon nanotubes using the hybrid nonlocal B3LYP function [8,47,48].

The reduction potential (^{Red}E) of 1 to 18 can be calculated using the Gibbs equation ($\Delta G = -nFE$) and the definition of adiabatic electron affinity. In this equation, ΔG is equal to the adiabatic electron affinity (the free energy of electron transfer, ΔG_{et} in J mol^{-1}, 1 eV = 96,471 J mol^{-1}, F = 96,495 coulomb, and n = 1). For example, the reduction potentials (^{Red}E) of $C_{20}H_{20}$ and $C_{30}H_{20}$ are equal to –0.34 and –0.89 V, respectively. The ^{Red}E of [SWCNT(5,5)-armchair-C_nH_{20}] (n = 20 to 190) 1 to 18 were calculated and are presented in Table 1. The amount of ^{Red}E (in V) = $-E_{aa}$ (in eV), where E_{aa} is the adiabatic electron affinity (see Table 1 for more details).

The values of the relative structural coefficients of the (5,5) armchair SWCNT for $C_{20}H_{20}$ up to $C_{190}H_{20}$ ([SWCNT(5,5)-armchair-C_nH_{20}], 1 to 18), the adiabatic electron affinity (E_{aa} in eV) and the reduction potentials (^{Red}E in V) of 1 to 18 are shown in Table 1. The absolute value of E_{aa} or ^{Red}E increases with the number of carbon atoms in 1 to 18. From $C_{20}H_{20}$ up to $C_{190}H_{20}$, the point groups alternate between D_{5d} and D_{5h} [9]. Using the equations 8 to 16 in Table 2, the values in Table 1, and the Rehm-Weller equation, we extended our results to compounds 19 to 29.

Table 1 The values of the coefficients of SWCNT 1 to 18 and the complexes 30 to 119

Number	Molecular formula	Point group	E_{aa} (eV)	^{Red}E (V)	[SWCNT][η^2-C_{60}Pd(dppf)]		[SWCNT][η^2-C_{60}Pd(dppr)]		[SWCNT][η^2-C_{60}Pd(dppcym)$_2$]		[SWCNT][η^2-C_{70}Pd(dppr)]		[SWCNT][η^2-C_{70}Pd(dppcym)$_2$]	
					(30 to 47)		(48 to 65)		(66 to 83)		(84 to 101)		(102 to 119)	
					$\Delta G_{et(1)}$	$\Delta G_{et(2)}$	$\Delta G_{et(1)}$	$\Delta G_{et(2)}$	$\Delta G_{et(1)}$	$\Delta G_{et(2)}$	$\Delta G_{et(1)}$	$\Delta G_{et(2)}$	$\Delta G_{et(1)}$	$\Delta G_{et(2)}$
1	$C_{20}H_{20}$	D_{5d}	0.34	−0.34	27.2108	35.2818	26.0578	33.8982	30.9004	40.3550	26.9802	34.8206	30.9004	38.2796
2	$C_{30}H_{20}$	D_{5h}	0.89	−0.89	39.8938	47.9648	38.7408	46.5812	43.5834	53.0380	39.6632	47.5036	43.5834	50.9626
3	$C_{40}H_{20}$	D_{5d}	0.67	−0.67	34.8206	42.8916	33.6676	41.5080	38.5102	47.9648	34.5900	42.4304	38.5102	45.8894
4	$C_{50}H_{20}$	D_{5h}	1.14	−1.14	45.6588	53.7298	44.5058	52.3462	49.3484	58.8030	45.4282	53.2686	49.3484	56.7276
5	$C_{60}H_{20}$	D_{5d}	1.56	−1.56	55.3440	63.4150	54.1910	62.0314	59.0336	68.4882	55.1134	62.9538	59.0336	66.4128
6	$C_{70}H_{20}$	D_{5h}	1.34	−1.34	50.2708	58.3418	49.1178	56.9582	53.9604	63.4150	50.0402	57.8806	53.9604	61.3396
7	$C_{80}H_{20}$	D_{5d}	1.61	−1.61	56.4970	64.5680	55.3440	63.1844	60.1866	69.6412	56.2664	64.1068	60.1866	67.5658
8	$C_{90}H_{20}$	D_{5h}	1.98	−1.98	65.0292	73.1002	63.8762	71.7166	68.7188	78.1734	64.7986	72.6390	68.7188	76.0980
9	$C_{100}H_{20}$	D_{5d}	1.71	−1.71	58.8030	66.8740	57.6500	65.4904	62.4926	71.9472	58.5724	66.4128	62.4926	69.8718
10	$C_{110}H_{20}$	D_{5h}	1.91	−1.91	63.4150	71.4860	62.2620	70.1024	67.1046	76.5592	63.1844	71.0248	67.1046	74.4838
11	$C_{120}H_{20}$	D_{5d}	2.24	−2.24	71.0248	79.0958	69.8718	77.7122	74.7144	84.1690	70.7942	78.6346	74.7144	82.0936
12	$C_{130}H_{20}$	D_{5h}	2.06	−2.06	66.8740	74.9450	65.7210	73.5614	70.5636	80.0182	66.6434	74.4838	70.5636	77.9428
13	$C_{140}H_{20}$	D_{5d}	2.13	−2.13	68.4882	76.5592	67.3352	75.1756	72.1778	81.6324	68.2576	76.0980	72.1778	79.5570
14	$C_{150}H_{20}$	D_{5h}	2.43	−2.43	75.4062	83.4772	74.2532	82.0936	79.0958	88.5504	75.1756	83.0160	79.0958	86.4750
15	$C_{160}H_{20}$	D_{5d}	2.35	−2.35	73.5614	81.6324	72.4084	80.2488	77.2510	86.7056	73.3308	81.1712	77.2510	84.6302
16	$C_{170}H_{20}$	D_{5h}	2.23	−2.23	70.7942	78.8652	69.6412	77.4816	74.4838	83.9384	70.5636	78.4040	74.4838	81.8630
17	$C_{180}H_{20}$	D_{5d}	2.53	−2.53	77.7122	85.7832	76.5592	84.3996	81.4018	90.8564	77.4816	85.3220	81.4018	88.7810
18	$C_{190}H_{20}$	D_{5h}	2.45	−2.45	75.8674	83.9384	74.7144	82.5548	79.5570	89.0116	75.6368	83.4772	79.5570	86.9362

[SWCNT(5,5)-armchair-C_nH_{20}] (n = 20 to 190) 1 to 18 and $\Delta G_{et(n)}$ (n = 1,2) of the complexes [SWCNT(5,5)-armchair-C_nH_{20}][R] (R = η^2-C_mPd(dppf), η^2-C_mPd(dppr), and η^2-C_mPd(dppcym)$_2$, n = 20 to 300 and m = 60 and 70) 30 to 119. Values for [SWCNT(5,5)-armchair-C_nH_{20}] (n = 20 to 190) 1 to 18 were calculated and reported at the 6-31G* level ([7] and calculated method in the text). The compounds [SWCNT(5,5)-armchair-C_nH_{20}][R] (R = η^2-C_mPd(dppf), η^2-C_mPd(dppr), and η^2-C_mPd(dppcym)$_2$, n = 20 to 300 and m = 60 and 70) supramolecular complexes 30 to 119 were not synthesized or reported. The data of $\Delta G_{et(n)}$ (n = 1 and 2, in kcal mol^{-1}) for supramolecular complexes 30 to 119 were calculated using the Rehm-Weller equation.

Equations 6 and 7 show the relationship between the number of carbon atoms (n) of [SWCNT(5,5)-armchair] and the adiabatic electron affinity (E_{aa} in eV) and reduction potential (^{Red}E in V) of [SWCNT(5,5)-armchair-C_nH_{20}] (n = 20 to 190) 1 to 18, respectively. Equation 6, like Equation 7, shows the *Nieperian* logarithmic behavior of the relationship. The R squared value (R^2) for the graphs was 0.9461.

$$E_{aa} = 22.417\mathrm{Ln}(n) - 66.853 \quad (6)$$

Table 2 The Nieperian relationship equations 8 to 16

Complexes of 1 to 18 with ligands A to E [SWCNT(5,5)-armchair-C_nH_{20}][R] (R = η^2-C_mPd(dppf), η^2-C_mPd(dppr), and η^2-C_mPd(dppcym)$_2$, n = 20 to 300 and m = 60 to 70)		Equation	R^2	$\Delta G_{et(n)} = a\ \mathrm{Ln}(n) + b$	
Stage (n)	Ligand[a]			a	b
1	A	8	0. 9461	22.416	40.789
2		9	0. 9461	22.416	32.718
1	B	10	0.9461	22.416	41.942
2		11	0.9461	22.416	34.102
1	C	12	0.9461	22.416	37.100
2		13	0.9461	22.416	27.645
1	D	14	0.9461	22.416	41.020
2		15	0.9461	22.416	33.180
1	E	16	0.9461	22.416	37.100

The said equations indicated the relationship between the number of carbon atoms in 1 to 18 and $\Delta G_{et(n)}$ (n = 1,2) of [SWCNT(5,5)-armchair-C_nH_{20}] (n = 20 to 190) 1 to 18. with η^2-C_mPd(dppf), η^2-C_mPd(dppr), and η^2-C_mPd(dppcym)$_2$(m = 60 and 70) (A to E) in the complexes [SWCNT(5,5)-armchair-C_nH_{20}][R] (R = η^2-C_mPd(dppf), η^2-C_mPd(dppr), and η^2-C_mPd(dppcym)$_2$, n = 20 to 300 and m = 60 and 70) 30 to 119. [a]The structures concerning these equations are shown in Figure 1.

$$^{Red}E = 0.9721\ \mathrm{Ln}(n) - 2.6088. \quad (7)$$

Using these equations, we derived a good approximation for extending the formulas for the E_{aa} and the ^{Red}E to [SWCNT(5,5)-armchair-C_nH_{20}] (n = 200 to 300) 19 to 29.

The relative structural coefficients, the E_{aa} (in eV), and the ^{Red}E (in V) of [SWCNT(5,5)-armchair-C_nH_{20}] (n = 20 to 190) 1 to 18 are found in Table 1. The relationship between this index and the first and second free energies of electron transfer ($\Delta G_{et(n)}$, n = 1,2), as assessed using the Rehm-Weller equation based on the first and second oxidation potentials ($^{ox}E_1$ and $^{ox}E_2$) of A to E for the predicted supramolecular complexes between 1 to 18 with the η^2–C_mPd(dppf), η^2–C_mPd(dppr), and η^2–C_mPd(dppcym)$_2$ (m = 60 and 70) ligands (A to E) as [SWCNT(5,5)-armchair-C_nH_{20}] (n = 20 to 190) 1 to 18 to produce [SWCNT(5,5)-armchair-C_nH_{20}][R] (R = η^2-C_mPd(dppf), η^2-C_mPd(dppr), and η^2-C_mPd(dppcym)$_2$, n = 20 to 300 and m = 60 and 70) 30 to 119, is presented.

Figure 2 shows the relationship between the number (n) of carbon atoms in the [SWCNT(5,5)-armchair] 1 to 18 and the first and second free energies of electron transfer ($\Delta G_{et(n)}$, n = 1,2 kcal mol^{-1}) of the ligands η^2–C_{60}Pd(dppf) (A). These data were fit using a regression with a second-order polynomial. The R^2 values for these graphs were 0.9461. We calculated the values of $\Delta G_{et(1)}$ and $\Delta G_{et(2)}$ of [SWCNT(5,5)-armchair-C_nH_{20}][η^2-C_{60}Pd(dppf)] (n = 20 to 190) 30 to 47 using equations 1, 8, and 9 (see Tables 1 and 2). The predicted values of $\Delta G_{et(n)}$ (n = 1,2) for [SWCNT(5,5)-armchair-C_nH_{20}][η^2-C_{60}Pd(dppf)] (n = 20 to 300) 30 to 47, and 120 to 130 were calculated using equations 8 and 9 (see Tables 2 and 3).

The first and second free energies of electron transfer ($\Delta G_{et(n)}$, n = 1,2 in kcal mol^{-1}) of the supramolecular complexes between the ligand η^2-C_{60}Pd(dppr) B and [SWCNT(5,5)-armchair-C_nH_{20}] (n = 20 to 190) 1 to 18 as presented [SWCNT(5,5)-armchair-C_nH_{20}][η^2-C_{60}Pd(dppr)] (n = 20 to 190) 48 to 65 are shown in Table 1. Equations 10 and 11 show the second-order polynomial behavior between the number of carbon atoms of 1 to 18 and the free energies of electron transfers in the supramolecular nanostructures of 48 to 65. Using these equations, we achieved a good approximation for extending the first and second free energies of electron transfer ($\Delta G_{et(n)}$; n = 1,2 in kcal mol^{-1}) for the other [SWCNT(5,5)-armchair-C_nH_{20}][η^2-C_{60}Pd(dppr)] (n = 200 to 300) 131 to 141. The R^2 values for the relationships were 0.9461. The predicted values of $\Delta G_{et(n)}$ (n = 1,2) for [SWCNT(5,5)-armchair-C_nH_{20}][η^2-C_{60}Pd(dppr)] (n = 200 to 300) 131 to 141 were calculated using equations 10 and 11 (see Tables 2 and 3). Tables 1 and 3 show that the values of the first and second free energies of electron transfer ($\Delta G_{et(n)}$, n = 1,2) increased in the supramolecular complexes of [SWCNT(5,5)-armchair-C_nH_{20}][η^2-C_{60}Pd(dppr)] (n = 20 to 300) 48 to 65 and 131 to 141 with increasing numbers of carbon atoms in the [SWCNT(5,5)-armchair-C_nH_{20}] structures.

The free energies of electron transfer ($\Delta G_{et(n)}$, n = 1,2 in kcal mol^{-1}) of the complexes between the ligand η^2–C_{60}Pd(dppcym)$_2$ C and [SWCNT(5,5)-armchair-C_nH_{20}] (n = 20

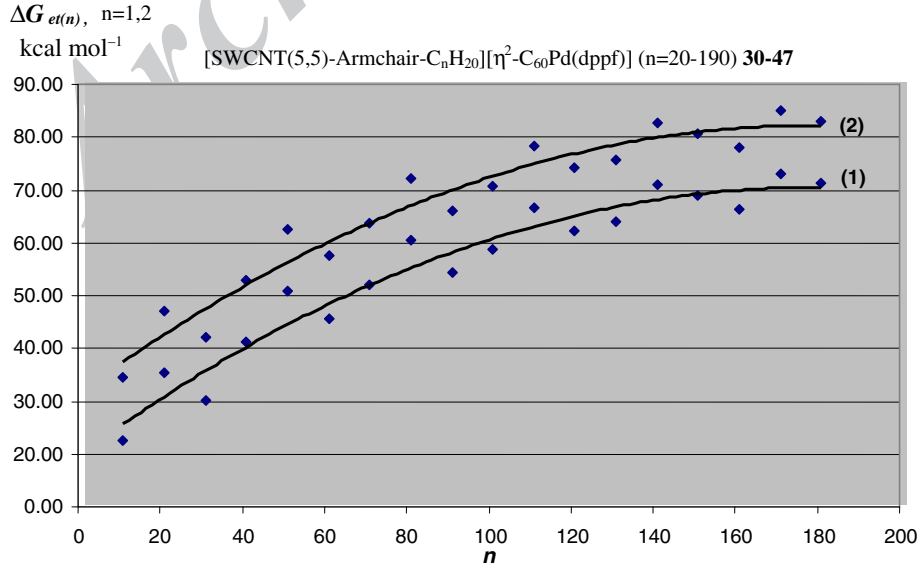

Figure 2 The relationship between the number of carbon atoms and free energies of ET. [SWCNT(5,5)-armchair-C_nH_{20}][η^2-C_{60}Pd(dppf)] complexes 30 to 47. The free energies of ET were calculated using the Rehm-Weller equation. The related curves for other complexes [SWCNT(5,5)-armchair-C_nH_{20}][η^2-C_{60}Pd(dppf)] (n = 20 to 190) 30 to 47 have similar structures with this figure.

Table 3 Values of the relative coefficients of SWCNT 19 to 29 and the complexes 120 to 174

Number	Molecular formula	Point group	Adiabatic electron affinity (eV)	^{Red}E (V)	[SWCNT][η^2-C_{60}Pd(dppf)] (120 to 130)		[SWCNT][η^2-C_{60}Pd(dppr)] (131 to 141)		[SWCNT][η^2-C_{60}Pd(dppcym)$_2$] (142 to 152)		[SWCNT][η^2-C_{70}Pd(dppr)] (153 to 163)		[SWCNT][η^2-C_{70}Pd(dppcym)$_2$] (164 to 174)	
					$\Delta G_{et(1)}$	$\Delta G_{et(2)}$	$\Delta G_{et(1)}$	$\Delta G_{et(2)}$	$\Delta G_{et(1)}$	$\Delta G_{et(2)}$	$\Delta G_{et(1)}$	$\Delta G_{et(2)}$	$\Delta G_{et(1)}$	$\Delta G_{et(2)}$
19	$C_{200}H_{20}$	D_{5d}	2.49	−2.49	76.7898	84.8608	75.6368	83.4772	80.4794	89.9340	76.5592	84.3996	80.4794	87.8586
20	$C_{210}H_{20}$	D_{5h}	2.53	−2.53	77.7122	85.7832	76.5592	84.3996	81.4018	90.8564	77.4816	85.3220	81.4018	88.7810
21	$C_{220}H_{20}$	D_{5d}	2.57	−2.57	78.6346	86.7056	77.4816	85.3220	82.3242	91.7788	78.4040	86.2444	82.3242	89.7034
22	$C_{230}H_{20}$	D_{5h}	2.60	−2.60	79.3264	87.3974	78.1734	86.0138	83.0160	92.4706	79.0958	86.9362	83.0160	90.3952
23	$C_{240}H_{20}$	D_{5d}	2.64	−2.64	80.2488	88.3198	79.0958	86.9362	83.9384	93.3930	80.0182	87.8586	83.9384	91.3176
24	$C_{250}H_{20}$	D_{5h}	2.67	−2.67	80.9406	89.0116	79.7876	87.6280	84.6302	94.0848	80.7100	88.5504	84.6302	92.0094
25	$C_{260}H_{20}$	D_{5d}	2.71	−2.71	81.8630	89.9340	80.7100	88.5504	85.5526	95.0072	81.6324	89.4728	85.5526	92.9318
26	$C_{270}H_{20}$	D_{5h}	2.74	−2.74	82.5548	90.6258	81.4018	89.2422	86.2444	95.6990	82.3242	90.1646	86.2444	93.6236
27	$C_{280}H_{20}$	D_{5d}	2.77	−2.77	83.2466	91.3176	82.0936	89.9340	86.9362	96.3908	83.0160	90.8564	86.9362	94.3154
28	$C_{290}H_{20}$	D_{5h}	2.80	−2.80	83.9384	92.0094	82.7854	90.6258	87.6280	97.0826	83.7078	91.5482	87.6280	95.0072
29	$C_{300}H_{20}$	D_{5d}	2.83	−2.83	84.6302	92.7012	83.4772	91.3176	88.3198	97.7744	84.3996	92.2400	88.3198	95.6990

[SWCNT(5,5)-armchair-C_nH_{20}] (n = 200 to 300) 19 to 29 and $\Delta G_{et(n)}$ (n = 1,2) of [SWCNT(5,5)-armchair-C_nH_{20}][R] (R = η^2-C_mPd(dppf), η^2-C_mPd(dppr), and η^2-C_mPd(dppcym)$_2$, n = 20 to 300, and m = 60 and 70) complexes 120 to 174.The compounds [SWCNT(5,5)-armchair-C_nH_{20}][R] (R = η^2-C_mPd(dppf), η^2-C_mPd(dppr), and η^2-C_mPd(dppcym)$_2$, n = 20 to 300 and m = 60 and 70) supramolecular complexes 120 to 174 were not synthesized or reported. The data of $\Delta G_{et(n)}$ (n = 1 and 2, in kcal mol^{-1}) for supramolecular complexes 120 to 174 were calculated using equations 8 to 16.The complexes 120 to 174 were not synthesized and reported previously.

to 190) 1 to 18, as presented in [SWCNT(5,5)-armchair-C_nH_{20}][η^2-C_{60}Pd(dppcym)$_2$] (n = 20 to 190) 66 to 83, are shown in Table 1. Equations 12 and 13 show the second-order polynomial relationship between the number of carbon atoms of 1 to 18 and the free energies of electron transfers at the supramolecular nanostructures of 66 to 83. Using these equations, we were able to extend the first and second free energies of electron transfer ($\Delta G_{et(n)}$ n = 1,2 in kcal mol^{-1}) for [SWCNT(5,5)-armchair-C_nH_{20}][η^2-C_{60}Pd(dppcym)$_2$] (n = 200 to 300) 142 to 152. The R^2 values for the relationships were 0.9461. The predicted values of $\Delta G_{et(n)}$ (n = 1,2) for [SWCNT(5,5)-armchair-C_nH_{20}][η^2-C_{60}Pd(dppcym)$_2$] (n = 200 to 300) 142 to 152 were calculated using equations 12 and 13 (Tables 2 and 3). The values of the first and second free energies of electron transfer ($\Delta G_{et(n)}$, n = 1,2) increased in the supramolecular complexes of [SWCNT(5,5)-armchair-C_nH_{20}][η^2-C_{60}Pd(dppcym)$_2$] (n = 20 to 300) 66 to 83 and 142 to 152 with increasing numbers of carbon atoms in the [SWCNT(5,5)-armchair-C_nH_{20}] structures (Tables 1 and 3).

The first and second free energies of electron transfer ($\Delta G_{et(n)}$, n = 1,2 in kcal mol^{-1}) of the supramolecular complexes between the ligands η^2-C_{70}Pd(dppr) D and η^2-C_{70}Pd(dppr) E with [SWCNT(5,5)-armchair-C_nH_{20}] (n = 20 to 190) 1 to 18 as presented in [SWCNT(5,5)-armchair-C_nH_{20}][η^2-C_{70}Pd(dppr)] and [SWCNT(5,5)-armchair-C_nH_{20}][η^2-C_{70}Pd(dppcym)$_2$] (n = 20 to 190) 84 to 101 and 102 to 119, respectively, are shown in Table 1. Equations 14 to 15 and 16 to 17 show the second-order polynomial relationship between the number of carbon atoms of 1 to 18 and the free energies of electron transfers in the 84 to 101 and 102 to 119 nanostructures. Using these equations, we extended the first and second free energies of electron transfer ($\Delta G_{et(n)}$, n = 1,2 in kcal mol^{-1}) for [SWCNT(5,5)-armchair-C_nH_{20}][η^2-C_{70}Pd(dppr)] and [SWCNT(5,5)-armchair-C_nH_{20}][η^2-C_{70}Pd(dppcym)$_2$] 153 to 163 and 164 to 174. The R^2 for the relationships were 0.9461. The predicted values of $\Delta G_{et(n)}$ (n = 1,2) for [SWCNT(5,5)-armchair-C_nH_{20}][η^2-C_{70}Pd(dppr)] and [SWCNT(5,5)-armchair-C_nH_{20}][η^2-C_{70}Pd(dppcym)$_2$] 153 to 163 and 164 to 174 were calculated using equations 14 to 15 and 16 to 17 (Tables 2 and 3, respectively). The values of the first and second free energies of electron transfer ($\Delta G_{et(n)}$, n = 1,2) increased in the supramolecular complexes of [SWCNT(5,5)-armchair-C_nH_{20}][η^2-C_{70}Pd(dppr)] and [SWCNT(5,5)-armchair-C_nH_{20}][η^2-C_{70}Pd(dppcym)$_2$] 84 to 119 and 153 to 174 with increasing numbers of carbon atoms in the [SWCNT(5,5)-armchair-C_nH_{20}] structures (Tables 1 and 3).

The Marcus theory is currently the dominant theory of electron transfer in chemistry. This theory is widely accepted because it accurately predicts electron transfer rates. The most significant prediction is that the rate of electron transfer will increase as the electron transfer reaction becomes more exergonic, but only to a point [37-42].

ET is one of the most important chemical processes in nature and plays a central role in many biological, physical, and chemical (both organic and inorganic) systems. Solid-state electronics depends on controlling ET in semiconductors. Current molecular electronics depends critically on understanding and controlling the transfer of electrons in and between molecules and nanostructures. Electron transfer is a very simple chemical reaction, which

can be used to gain insight into other kinds of chemistry and biochemistry. Electron transfer is fundamental in chemistry [37-42].

The free energy of electron transfer ΔG_{et} is the difference between the reactants and the products, and $\Delta G^{\#}_{et}$ is the activation energy. The reorganization energy is the energy required to force the reactants to have the same nuclear configuration as the products without permitting the electron transfer. If the entropy changes are ignored, the free energy becomes energy or potential energy [37-42].

Using Equation 2, we calculated the first and second activation free energies of electron transfer, $\Delta G^{\#}_{et(n)}$, for 30 to 174 in accordance with the Marcus theory; see Table 4. Figure 3 shows the surfaces of the free energies of electron transfer $\Delta G_{et(n)}$ and $\Delta G^{\#}_{et(n)}$ (n = 1,2) between [SWCNT (5,5)-armchair-C_nH_{20}] (n = 20 to 300) 1 to 29 and the ligands η^2–C_mPd(dppf), η^2–C_mPd(dppr), and η^2–C_mPd $(dppcym)_2$ (m = 60 and 70) A to E to produce [SWCNT (5,5)-armchair-C_nH_{20}][R] (R = η^2-C_mPd(dppf), η^2-C_mPd (dppr), and η^2-C_mPd$(dppcym)_2$, n = 20 to 300 and m = 60 and 70) 30 to 174. The values of the first and second activation free energies of electron transfer $\Delta G^{\#}_{et(n)}$ (n = 1,2) for 30 to 174 increased with increasing $\Delta G_{et(n)}$ and the numbers of carbon atoms in the complexes, while the

Table 4 The values of the first and second free activation energies of electron transfer

Number of SWCNT(5,5)-armchair-C_nH_{20}	[SWCNT][η^2-C_{60} Pd(dppf)]		[SWCNT][η^2-C_{60} Pd(dppr)]		[SWCNT][η^2-C_{60} $Pd(dppcym)_2$]		[SWCNT][η^2-C_{70} Pd(dppr)]		[SWCNT][η^2-C_{70} $Pd(dppcym)_2$]	
	(30 to 47)		(48 to 65)		(66 to 83)		(84 to 101)		(102 to 119)	
	$\Delta G^{\#}_1$	$\Delta G^{\#}_2$	$\Delta G^{\#}_1$	$\Delta G^{\#}_2$	$\Delta G^{\#}_1$	$\Delta G^{\#}_2$	$\Delta G^{\#}_1$	$\Delta G^{\#}_2$	$\Delta G^{\#}_1$	$\Delta G^{\#}_2$
1	35.9794	53.6851	33.7382	50.3991	43.6353	66.6218	35.5254	52.5782	43.6353	61.1609
2	65.3881	88.6426	62.3542	84.4054	75.5806	105.0671	64.7755	87.2187	75.5806	98.1794
3	52.5782	73.6133	49.8615	69.7565	61.7561	88.6426	52.0291	72.3162	61.7561	82.3256
4	81.6382	107.4149	78.2440	102.7453	92.9837	125.4248	80.9536	105.8468	92.9837	117.8885
5	112.9940	143.0080	108.9945	137.6120	126.2766	163.6813	112.1883	141.1978	126.2766	155.0554
6	95.9354	123.7299	92.2530	118.7143	108.2033	143.0080	95.1931	122.0465	108.2033	134.9529
7	117.0655	147.5840	112.9940	142.1015	130.5787	168.5744	116.2455	145.7450	130.5787	159.8188
8	149.4346	183.6859	144.8298	177.5634	164.6542	207.0226	148.5078	181.6335	164.6542	197.3071
9	125.4248	156.9521	121.2091	151.2967	139.3991	178.5766	124.5759	155.0554	139.3991	169.5616
10	143.0080	176.5531	138.5041	170.5518	157.9048	199.4459	142.1015	174.5411	157.9048	189.9121
11	174.5411	211.4155	169.5616	204.8434	190.9599	236.4010	173.5395	209.2133	190.9599	226.0111
12	156.9521	192.0105	152.2320	185.7497	172.5407	215.8546	156.0023	189.9121	172.5407	205.9316
13	163.6813	199.4459	158.8603	193.0641	179.5927	223.7339	162.7114	197.3071	179.5927	213.6293
14	194.1205	232.9118	188.8672	226.0111	211.4155	259.1022	193.0641	230.6000	211.4155	248.2193
15	185.7497	223.7339	180.6117	216.9715	202.6758	249.4170	184.7164	221.4682	202.6758	238.7416
16	173.5395	210.3130	168.5744	203.7582	189.9121	235.2351	172.5407	208.1165	189.9121	224.8710
17	204.8434	244.6435	199.4459	237.5699	222.5996	271.4681	203.7582	242.2741	222.5996	260.3258
18	196.2420	235.2351	190.9599	228.2998	213.6293	261.5523	195.1798	232.9118	213.6293	250.6175
19	200.5197	239.9162	195.1798	232.9118	218.0914	266.4871	199.4459	237.5699	218.0914	255.4486
20	204.8434	244.6435	199.4459	237.5699	222.5996	271.4681	203.7582	242.2741	222.5996	260.3258
21	209.2133	249.4170	203.7582	242.2741	227.1540	276.4952	208.1165	247.0245	227.1540	265.2491
22	212.5210	253.0273	207.0226	245.8326	230.6000	280.2957	211.4155	250.6175	230.6000	268.9718
23	216.9715	257.8814	211.4155	250.6175	235.2351	285.4035	215.8546	255.4486	235.2351	273.9759
24	220.3397	261.5523	214.7405	254.2365	238.7416	289.2646	219.2141	259.1022	238.7416	277.7591
25	224.8710	266.4871	219.2141	259.1022	243.4574	294.4531	223.7339	264.0139	243.4574	282.8439
26	228.2998	270.2185	222.5996	262.7817	247.0245	298.3748	227.1540	267.7280	247.0245	286.6877
27	231.7544	273.9759	226.0111	266.4871	250.6175	302.3224	230.6000	271.4681	250.6175	290.5574
28	235.2351	277.7591	229.4484	270.2185	254.2365	306.2959	234.0720	275.2341	254.2365	294.4531
29	238.7416	281.5684	232.9118	273.9759	257.8814	310.2954	237.5699	279.0260	257.8814	298.3748

[SWCNT(5,5)-armchair-C_nH_{20}][R] (R = η^2-C_mPd(dppf), η^2-C_mPd(dppr), and η^2-C_mPd$(dppcym)_2$, n = 20 to 190 and m = 60 and 70) complexes 30 to 119, between 1 to 18 and A to E.

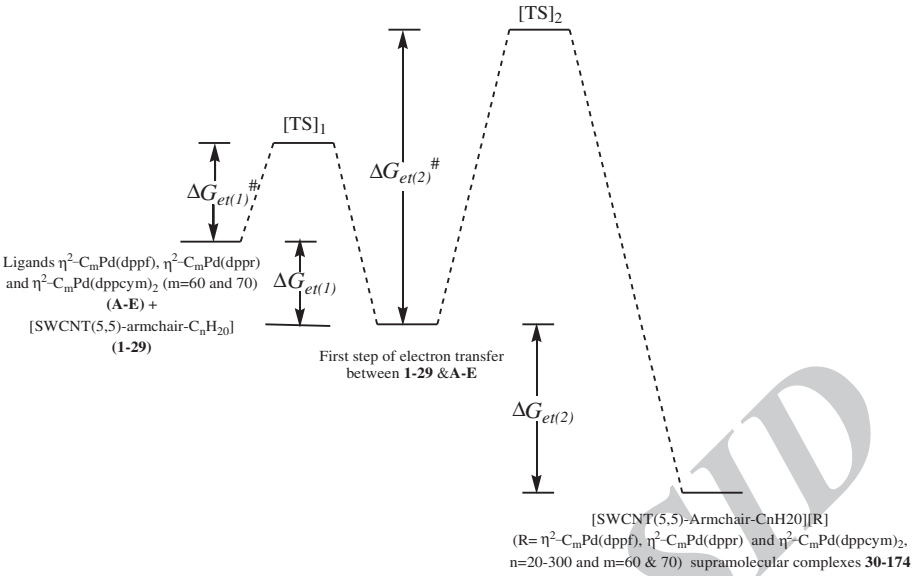

Figure 3 The values of $\Delta G_{et(n)}$ and $\Delta G^{\#}_{et(n)}$ of ET between 1 to 29 and A to E in the structures 30 to 174.

kinetic rate constants of the electron transfers decreased with increasing $\Delta G_{et(n)}$ and $\Delta G^{\#}_{et(n)}$ (n = 1,2) (see Tables 1, 3, and 4, and Figure 3).

Because of the good linear correlations between $\Delta G_{et(n)}$ (n = 1,2), E_{aa} and ^{Red}E of 1 to 18 with the ligands A to E, we used the values of E_{aa} and ^{Red}E to calculate the free energies of electron transfer (ΔG_{et} in kcal mol^{-1}) of [SWCNT(5,5)-armchair-C_nH_{20}] (n = 20 to 190) 1 to 18 to produce [SWCNT(5,5)-armchair-C_nH_{20}][R] (R = η^2-C_mPd(dppf), η^2-C_mPd(dppr), and η^2-C_mPd(dppcym)$_2$, m = 60 and 70) n = 20 to 190, 30 to 119, and n = 200 to 300, 120 to 174. The electron affinity and reduction potential have the same magnitude with opposite signs. The free energy of electron transfer can be calculated with the Rehm-Weller equation, which we determined was linearly dependent on the electron affinity of the compounds studied here. In Tables 1 and 3, the values of the first and second free energies of electron transfer ($\Delta G_{et(n)}$, n = 1,2) obtained for supramolecular complexes 30 to 119 and 120 to 174 from equations 8 to 17 (Table 2) are compared with those obtained with the Rehm-Weller equation.

The number of carbon atoms (n), E_{aa}, ^{Red}E, and $\Delta G_{et(n)}$ (n = 1,2) of [SWCNT(5,5)-armchair-C_nH_{20}] (n = 20 to 300) 1 to 29 and their complexes with the ligands η^2-C_mPd(dppf), η^2-C_mPd(dppr), and η^2-C_mPd(dppcym)$_2$ (m = 60 and 70) (A to E) as [SWCNT(5,5)-armchair-C_nH_{20}][R] (R = η^2-C_mPd(dppf), η^2-C_mPd(dppr), and η^2-C_mPd(dppcym)$_2$, n = 200 to 300 and m = 60 and 70) supramolecular complexes 120 to 174 are shown in Table 3. The ^{Red}E were extended for $C_{200}H_{20}$ up to $C_{300}H_{20}$ ([SWCNT(5,5)-armchair-C_nH_{20}], 19 to 29). The calculated results for ^{Red}E as well as the free energies of electron transfer ($\Delta G_{et(n)}$, n = 1, 2, in kcal mol^{-1}) according to the Rehm-Weller equation between A to E with 19 to 29 in structures 120 to 174 are presented in Table 3.

As shown in Figure 2, the periodicity of the plotted points is 3, which is common among benzenoids. Using Equation 1 (Rehm-Weller equation) and equations 2 to 17, the values of E_{aa}, ^{Red}E, $\Delta G_{et(n)}$ (n = 1,2), $\Delta G^{\#}_{et(n)}$, and $k_{et(n)}$ (n = 1,2) for 30 to 174 were calculated. The number of carbon atoms showed a good relationship with the values of the E_{aa}, the ^{Red}E of [SWCNT(5,5)-armchair-C_nH_{20}] (n = 20 to 190) 1 to 18 and 19 to 29, and the ΔG_{et} in [SWCNT(5,5)-armchair-C_nH_{20}][R] (R = η^2-C_mPd(dppf), η^2-C_mPd(dppr), and η^2-C_mPd(dppcym)$_2$, n = 20 to 300 and m = 60 and 70) supramolecular complexes 30 to 174. Figure 3 shows the free energy surfaces of electron transfer $\Delta G_{et(n)}$ and $\Delta G^{\#}_{et(n)}$ (n = 1,2) between 1 to 29 and the ligands A to E in the structures of 30 to 174, which were calculated using equations 1 to 17 and are shown in Tables 1, 2, 3, 4, and 5. With the appropriate equations, we calculated the E_{aa}, the ^{Red}E in 1 to 18 and 19 to 29, the first and second free energies of electron transfer (ΔG_{et} in kcal mol^{-1}), and the first and second activation free energies of electron transfer $\Delta G^{\#}_{et(n)}$ for 30 to 174 in accordance with the Marcus theory.

We determined the values of the maximum wavelengths ($\lambda_{(n)}$; n = 1 or2, in nm) for each stage of the electron transfer process in the nanostructure supramolecular complexes 30 to 174 with Planck's formula. Using this formula, we also determined the activation free energy of the electron transfer process. Most of the values were found in the UV–vis (190 to 800 nm) range of the

Table 5 Values of the first and the maximum wave lengths for each stage of the ET process

Number of SWCNT (5,5)-armchair-C_nH_{20}	Molecular formula	[SWCNT][η^2-C_{60}Pd (dppf)]		[SWCNT][η^2-C_{60}Pd (dppr)]		[SWCNT][η^2-C_{60}Pd (dppcym)$_2$]		[SWCNT][η^2-C_{70}Pd (dppr)]		[SWCNT][η^2-C_{70}Pd (dppcym)$_2$]	
		$\lambda_{(1)}$	$\lambda_{(2)}$	$\lambda_{(1)}$	$\lambda_{(2)}$	$\lambda_{(1)}$	$\lambda_{(2)}$	$\lambda_{(1)}$	$\lambda_{(2)}$	$\lambda_{(1)}$	$\lambda_{(2)}$
1	$C_{20}H_{20}$	794	532	847	567	655	429	804	543	655	467
2	$C_{30}H_{20}$	437	322	458	339	378	272	441	328	378	291
3	$C_{40}H_{20}$	543	388	573	410	463	322	549	395	463	347
4	$C_{50}H_{20}$	350	266	365	278	307	228	353	270	307	242
5	$C_{60}H_{20}$	253	200	262	208	226	175	255	202	226	184
6	$C_{70}H_{20}$	298	231	310	241	264	200	300	234	264	212
7	$C_{80}H_{20}$	244	194	253	201	219	169	246	196	219	179
8	$C_{90}H_{20}$	191	156	197	161	174	138	192	157	174	145
9	$C_{100}H_{20}$	228	182	236	189	205	160	229	184	205	169
10	$C_{110}H_{20}$	200	162	206	168	181	143	201	164	181	150
11	$C_{120}H_{20}$	164	135	169	139	150	121	165	137	150	126
12	$C_{130}H_{20}$	182	149	188	154	166	132	183	150	166	139
13	$C_{140}H_{20}$	175	143	180	148	159	128	176	145	159	134
14	$C_{150}H_{20}$	147	123	151	126	135	110	148	124	135	115
15	$C_{160}H_{20}$	154	128	158	132	141	115	155	129	141	120
16	$C_{170}H_{20}$	165	136	169	140	150	121	166	137	150	127
17	$C_{180}H_{20}$	139	117	143	120	128	105	140	118	128	110
18	$C_{190}H_{20}$	146	121	150	125	134	109	146	123	134	114
19	$C_{200}H_{20}$	142	119	146	123	131	107	143	120	131	112
20	$C_{210}H_{20}$	139	117	143	120	128	105	140	118	128	110
21	$C_{220}H_{20}$	137	115	140	118	126	103	137	116	126	108
22	$C_{230}H_{20}$	134	113	138	116	124	102	135	114	124	106
23	$C_{240}H_{20}$	132	111	135	114	121	100	132	112	121	104
24	$C_{250}H_{20}$	130	109	133	112	120	99	130	110	120	103
25	$C_{260}H_{20}$	127	107	130	110	117	97	128	108	117	101
26	$C_{270}H_{20}$	125	106	128	109	116	96	126	107	116	100
27	$C_{280}H_{20}$	123	104	126	107	114	95	124	105	114	98
28	$C_{290}H_{20}$	121	103	125	106	112	93	122	104	112	97
29	$C_{300}H_{20}$	120	101	123	104	111	92	120	102	111	96

The values are calculated using the *Plank's* formula. The wavelengths of [SWCNT(5,5)-armchair-C_nH_{20}][*R*] (*R* = η^2-C_mPd(dppf), η^2-C_mPd(dppr), and η^2-C_mPd(dppcym)$_2$, *n* = 20 to 300 and *m* = 60 to 70 30 to 174.

electromagnetic spectrum. The maximum wavelengths ($\lambda_{(n)}$; *n* = 1 or 2) depended on the $\Delta G^{\#}_{et(n)}$ value in each stage (Equation 4 and Table 5).

The supramolecular complexes of armchair single-wall nanotubes [SWCNT(5,5)-armchair-C_nH_{20}] (*n* = 20 to 300) 1 to 18 and 19 to 29 with the ligands η^2–C_mPd(dppf), η^2–C_mPd(dppr), and η^2–C_mPd(dppcym)$_2$ (*m* = 60 and 70) (A to E), i.e., [SWCNT(5,5)-armchair-C_nH_{20}][*R*] (*R* = η^2-C_mPd(dppf), η^2-C_mPd(dppr), and η^2-C_mPd(dppcym)$_2$, *n* = 20 to 300 and *m* = 60 and 70), and the calculated values of $\Delta G_{et(n)}$, $\Delta G^{\#}_{et(n)}$, and $\lambda_{(n)}$ (*n* = 1 and 2) corresponding to the supramolecular complexes 30 to 174 have neither been synthesized nor reported before.

Conclusions

The complexes η^2–C_mPd(dppf), η^2–C_mPd(dppr), and η^2–C_mPd(dppcym)$_2$ (*m* = 60 and 70) (A to E) contain a strongly electron-withdrawing fullerene cage and a metallocene group, which can be either electron releasing (ruthenocene) or electron withdrawing (cymantrene) and is linked with the cage through a bisdiphenyl phosphinepalladium bridge. The oxidation potentials

($^{ox}E_1$ and $^{ox}E_2$) of η^2–C_mPd(dppf), η^2–C_mPd(dppr), and η^2–C_mPd(dppcym)$_2$ (m = 60 and 70) (A to E) have been reported. In this study, we identified structural relationships between the number of carbon atoms and the E_{aa}, the values of the ^{Red}E of [SWCNT(5,5)-armchair-C_nH_{20}] (n = 20 to 300) 1 to 18 and 19 to 29, the $\Delta G_{et(n)}$, and the $\Delta G^{\#}_{et(n)}$ for the complexes 30 to 174. The number of carbon atoms is strongly correlated with the values of E_{aa} and ^{Red}E in the (5,5) armchair SWCNT 1 to 18 and 19 to 29, which are important factors in characterizing these materials. The values of $\Delta G_{et(n)}$ and $\Delta G^{\#}_{et(n)}$ (n = 1,2) were calculated using the Rehm-Weller equation and Equations 2 and 3 for 30 to 119 and 120 to 174 supramolecular nanostructure complexes, respectively. The maximum wavelengths of the electromagnetic photons in the photoelectron transfer process for each stage ($\lambda_{(n)}$; n = 1 to 2, in nm) of the nanostructure complexes 30 to 174 were calculated with Planck's equation. The novel supramolecular complexes and the calculated values have neither been synthesized nor reported previously. Using this model and the associated equations, we can easily calculate the E_{aa}, ^{Red}E, $\Delta G_{et(n)}$, $\Delta G^{\#}_{et(n)}$ (kcal mol^{-1}), and $\lambda_{(n)}$ (n = 1,2; in nm) of this family of compounds 30 to 174 with good approximation.

Competing interests
The authors declare that they have no competing interests.

Authors' contributions
AAT carried out the ET investigations. This study was a part of AAT's studies in ET process between important molecules and nanostructures. ZTH participated in the statistical analysis and background part of the study. All authors read and approved the final manuscript.

Authors' information
AAT is professor of Organic Chemistry and is an academic member of the Razi University (Kermanshah-Iran) since 2012. He was the academic member of Islamic Azad University (IAU), Arak, Iran from 1998 to 2012. AAT has spent his post-doctorate at The University of Queensland (UQ), Brisbane, Australia in Reactive Intermediates and Unusual Molecules Group under the supervision of Professor Curt Wentrup in Brisbane, Australia during 2006 and 2007. He has as well developed his scientific activities in Professor Curt Wentrup's laboratory at The University of Queensland and under his supervision in July to September of 2008 and August to September of 2009. Professor AAT has worked in The University of New England (UNE), Armidale, NSW, Australia with a sabbatical opportunity with Professor Stephen Glover's group from 2011 to 2012. AAT has won national prizes for his scientific paper (ISI, ISC, educational and propagation publication), books, invention, scientific activities, and conferences papers until now. AAT is one of the Members of the Central Committee of the Iranian Chemical Society (CCICS). ZTH has masters degree in Organic Chemistry from Islamic Azad University (IAU), Arak, Iran in 2011. ZTH has studied on theoretical electron transfer process between the exohedral metallofullerenes of Pd and SWCNT(5,5)-armchair nanotubes under the supervision of AAT.

Acknowledgments
The corresponding author gratefully acknowledges his colleagues in the Chemistry Department of The University of New England (UNE), Australia for their useful suggestions.

Author details
[1]Department of Organic Chemistry, Faculty of Chemistry, Razi University, P.O. Box 67149–67346, Kermanshah, Iran. [2]Chemistry Department, Faculty of Science, Islamic Azad University, P.O. Box 38135–567, Arak, Iran.

Received: 20 March 2012 Accepted: 5 March 2013
Published: 10 April 2013

References
1. Magdesieva, TV, Bashilov, VV, Kravchuk, DN, Dolgushin, FM, Butin, KP, Sokolov, VI: Comparison of electrochemical behavior of exohedral palladium complexes with [60]- and [70]-fullerenes and metallocene ligands. Russ. Chem. Bull. Int. Ed. **53**(4), 795–799 (2004)
2. Sokolov, VI: Fullerenes as a new type of ligands for transition metals. Russ. J. Coord. Chem. **33**(10), 711–724 (2007)
3. Fagan, PJ, Calabrese, JC, Malone, B: The chemical nature of buckminsterfullerene (C60) and the characterization of a platinum derivative. Science **252**, 1160 (1991)
4. Denisovich, LI, Peregudova, SM, Novikov, YN: Electrochemical properties of transition metal complexes with C60 and C70 fullerene ligands. Russ. J. Electrochem. **46**(1), 3–20 (2010)
5. Bashilov, VV, Magdesieva, TV, Kravchuk, DN, Petrovskii, PV, Ginzburg, AG, Butin, KP, Sokolov, VI: A new heterobimetallic palladium–[60] fullerene complex with bidentate bis-1,1′-[P]2-ferrocene ligand J. Organomet. Chem. **599**, 37 (2000)
6. Bashilov, VV, Petrovski, PV, Sokolov, VI: Synthesis of the first optically active organometallic fullerene derivative by η^2 functionalization of buckminsterfullerene by Pd(0) complexes. Russ. Chem. Bull. **42**, 392–393 (1993)
7. Yanilkin, VV, Gubskaya, VP, Nuretdinov, IA: Electrochemical synthesis of a phosphorylated monomethano [60] fullerene. Mendeleev Commun. **13**, 13–14 (2003)
8. Magdesieva, TV, Kravchuk, DN, Bashilov, VV, Kuznetsova, IV, Sokolov, VI, Butin, KP: Metalation of fullerenes: electrochemical synthesis and voltammetric study of heterometallic C60 and C70 complexes. Russ. Chem. Bull. Int. Ed. **51**, 1588 (2002)
9. Zhou, Z, Steigerwald, M, Hybertsen, M, Brus, L, Friesner, RA: Electronic structure of tubular aromatic molecules derived from the metallic (5,5) armchair single wall carbon nanotube. J. Am. Chem. Soc. **126**(11), 3597–3607 (2004)
10. Srivastava, D, Menon, M, Cho, K: Computational nanotechnology with carbon nanotubes and fullerenes. Comput. Sci. Eng. **3**, 42–55 (2001)
11. Lourie, O, Cox, DM, Wagner, HD: Buckling and collapse of embedded carbon nanotubes. Phys. Rev. Lett. **81**, 1638–1641 (1998)
12. Nagase, S, Kobayashi, K: The ionization energies and electron affinities of endohedral metallofullerenes MC82 (M = Sc, Y, La): density functional calculations. J. Chem. Soc. Chem. Commun. **16**, 1837–1838 (1994)
13. Dubois, D, Kadish, KM, Flanagan, S, Wilson, LJ: Electrochemical detection of fulleronium and highly reduced fulleride ($C60^{5-}$) ions in solution. J. Am. Chem. Soc. **113**(20), 7773–7774 (1991)
14. Xie, Q, Pérez-Cordero, E, Echegoyen, L: Electrochemical detection of $C60^{6-}$ and $C70^{6-}$: enhanced stability of fullerides in solution. J. Am. Chem. Soc. **114**(10), 3978–3980 (1992)
15. Li, Q, Wudl, F, Thilgen, C, Whetten, RL, Diederich, F: The unusual electrochemical properties of the higher fullerene, chiral C76. J. Am. Chem. Soc. **114**(10), 3994–3996 (1992)
16. Arellano, JS, Molina, LM, Rubio, A, Lopez, MJ, Alonso, JA: Interaction of molecular and atomic hydrogen with (5,5) and (6,6) single-wall carbon nanotubes. J. Chem. Phys. **117**(5), 2281–2288 (2002)
17. Srivastava, D, Barnard, S: Molecular dynamics simulation of large scale carbon nanotubes on shared memory architecture. Proc. IEEE Supercomputing, ACM/IEEE 1997 Conference, pp. 35. IEEE Computer Society Press, Los Alamitos, CA, USA (1997)
18. Yakobson, BI, Brabec, CJ, Bernholc, J: Nanomechanics of carbon tubes: instabilities beyond linear response. Phys. Rev. Lett. **76**, 2511–2514 (1996)
19. Dresselhaus, MS, Dresselhaus, G, Eklund, PC: Science of Fullerenes and Carbon Nanotubes. Academic, New York (1996)
20. Dai, H: Carbon nanotubes: synthesis, integration, and properties. Acc. Chem. Res. **35**(12), 1035–1044 (2002)
21. Collins, PG, Avouris, P: Nanotubes for electronics. Sci. Am. **283**, 38–45 (2000)
22. Dresselhaus, MS, Dresselhaus, G, Saito, R: Carbon fibers based on Ceo and their symmetry. Phys. Rev. B **45**(11), 6234–6242 (1992)

23. Mintmire, JW, Dunlap, BI, White, CT: Are fullerene tubules metallic? Phys. Rev. Lett. **68**(5), 631–634 (1992)
24. Barnett, R, Demler, E, Kaxiras, E: Electron–phonon interaction in ultrasmall-radius carbon nanotubes. Solid State Comm. **135**(5), 335–339 (2005)
25. Diudea, MV: Nanoporous carbon allotropes by septupling map operations. J. Chem. Inf. Model. **45**, 1002–1009 (2005)
26. Srivastava, D, Atluri, SN: Computational nanotechnology: a current perspective. Comput. Model. Eng. Sci. **3**(5), 531–538 (2002)
27. Bandow, S, Takizawa, M, Kato, H, Okazaki, T, Shinohara, H, Iijima, S: Smallest limit of tube diameters for encasing of particular fullerenes determined by radial breathing mode Raman scattering. Chem. Phys. Lett. **347**(1–3), 23–28 (2001)
28. Taherpour, AA: Quantitative structural relationship and theoretical study of electrochemical properties of C60@[SWCN(5, 5)-Armchair-CnH20] complexes. Chem. Phys. Lett. **469**, 135–139 (2009)
29. Taherpour, AA: Theoretical and quantitative structural relationship study of the electrochemical properties of [M2@Cx]@[SWCNT(5,5)-armchair-CnH20] (M = Er and Sc, x = 82 and 84, and n = 20–300) complexes. J. Phys. Chem. C. **113**, 5402–5408 (2009)
30. Taherpour, AA: Theoretical and quantitative structural relationships of the electrochemical and electron transfer properties of [M_x@C82]@[SWCNT(5,5)-armchair-C*n*H20] (x = 0, 1; for x = 1: M = Ce & Gd and n = 20–300) nanostructure complexes. Chem. Phys. Lett. **483**, 233–240 (2009)
31. Hansen, PJ, Jurs, P: Chemical applications of graph theory. Part I. Fundamentals and topological indices. J. Chem. Educ. **65**(7), 574–580 (1988)
32. Hosoya, H: Topological index. A newly proposed quantity characterizing the topological nature of structural isomers of saturated hydrocarbons. Bull. Chem. Soc. **44**, 2332–2339 (1971). Jpn
33. Randić, M: On characterization of molecular attributes. Acta. Chim. Slov. **45**(3), 239–252 (1998)
34. Du, YP, Liang, YZ, Li, BY, Xu, CJ: Orthogonalization of block variables by subspace projection for quantitative structure property relationship (QSPR) research. J. Chem. Inf. Cmput. Sci. **42**(5), 993–1003 (2002)
35. Bolboaca, SD, Jantschi, L: How good can the characteristic polynomial be for correlations? Int. J. Mol. Sci. **8**(4), 335–345 (2007)
36. Rehm, D, Weller, A: Kinetics of fluorescence quenching by electron and H-atom transfer Isr. J. Chem. **8**, 259–271 (1970)
37. Marcus, RA: Electron transfer reactions in chemistry: theory and experiment. Rev. Modern. Phys. **65**(3), 599–610 (1993)
38. Andrea, M: Marcus theory for electron transfer a short introduction MPIP. J. Club-Mainz. **1**, 1–13 (2008)
39. Barbara, PF, Meyer, TJ, Ratner, MA: Contemporary issues in electron transfer research. J. Phys. Chem. **100**(31), 13148–13168 (1996)
40. Newton, MD: Quantum chemical probes of electron-transfer kinetics: the nature of donor-acceptor interactions. Chem. Rev. **91**, 767–792 (1991)
41. Marcus, RA, Sutin, N: Electron transfer in Chemistry and Biology. Biochim. Biophys. Acta. **811**, 265 (1985)
42. Kuzmin, MG: What defines the activation energy of electron transfer: reorganization energy or electron coupling? XVIIth IUPAC Symposium on Photochemistry. (2000). 22–27 July
43. Atkins, PW: Physical Chemistry, 6th edn. Oxford University Press, Oxford (1998)
44. Minkin, VI: Glossary of terms used in theoretical organic chemistry. Pure. Appl. Chem. **71**(10), 1919–1981 (1999)
45. Zhang, LY, Friesner, RA: Ab initio electronic structure calculation of the redox potentials of bacteriochlorophyll and bacteriopheophytin in solution. J. Phys. Chem. **99**(44), 16479–16482 (1995)
46. Topol, IA, McGrath, C, Chertova, E, Dasenbrock, C, Lacourse, WR, Eissenstat, MA, Burt, SK, Henderson, LE, Casas-Finet, JR: Experimental determination and calculations of redox potential descriptors of compounds directed against retroviral zinc fingers: implications for rational drug design. Protein. Sci. **10**(7), 1434–1445 (2001)
47. Becke, AD: Density--functional thermochemistry. III. The role of exact exchange. J. Chem. Phys. **98**(7), 5648–5652 (1993)
48. Curtiss, LA, Raghavachari, K: Addendum to Gaussian-3 and related methods for accurate thermochemistry. Theor. Chem. Acc. **108**, 61–70 (2002)

doi:10.1186/2228-5326-3-22
Cite this article as: Taherpour and Talebi-Haftadori: **Free energies, kinetics, and photoelectron-transfer properties, and theoretical and quantitative structural relationship studies of [SWCNT(5,5)-armchair-C_nH_{20}][*R*] (*R* = η^2-C_mPd(dppf), η^2-C_mPd(dppr), and η^2-C_mPd(dppcym)$_2$, n = 20 to 300 and m = 60 and 70) nanostructure complexes.** *International Nano Letters* 2013 **3**:22.